Research papers

Experimental smelting of iron ores from Elba Island (Tuscany, Italy): Results and implications for the reconstruction of ancient metallurgical processes and iron provenance

M. Benvenuti [a, b, *], A. Orlando [b], D. Borrini [a], L. Chiarantini [b], P. Costagliola [a], C. Mazzotta [a], V. Rimondi [a]

[a] Dipartimento di Scienze della Terra, University of Firenze, Via G. La Pira 4, 50121 Florence, Italy
[b] CNR-Istituto di Geoscienze e Georisorse, Via G. La Pira 4, 50121 Florence, Italy

A B S T R A C T

Iron deposits from Elba Island (Tuscan Archipelago) were extensively exploited since the 1st millennium BC: both raw iron ore and smelted blooms were extensively traded through the Mediterranean region. Within the frame of the multidisciplinary research Project "AITHALE" (from the Greek name for Elba Island), we have performed a series of archaeometallurgical experiments primarily to investigate the traceability of Elban iron ores during the various steps of the *chaîne opératoire* of bloomery iron production. Results of experiments performed both in the field (reconstruction of a bloomery furnace) and in the laboratory (smelting experiments carried out in a gas mixing furnace) are discussed in the text. Slags produced by smelting of W-Sn-rich iron (hematite) ores, like those from Elba island, show the presence of these elements in phases of their own, either relic (scheelite, ferberite, cassiterite) and/or newly formed (iron-tin alloys). Iron bloom obtained from this kind of iron ore could also bear evidence of the peculiar geochemistry of smelted ore, with tungsten preferentially associated with slag inclusions and tin eventually enriched in the metallic phase.

© 2016 Elsevier Ltd. All rights reserved.

1. Introduction

One of the main targets of the research project "AITHALE" (from the ancient Greek name for Elba Island) is the characterization of the three-millennia-long mining and metallurgical processing of ore deposits from Elba Island across the whole Mediterranean area, with particular reference to the pre-Modern periods, from the 1st millennium BC up to the Middle Ages (cf. Corretti et al., 2014).

Notwithstanding many decades of archaeological research in the ancient territory of Etruria, our knowledge about technological aspects of iron smelting in Etruscan and Roman periods is still very tenuous and fragmentary (cf. Corretti and Benvenuti, 2001; Benvenuti et al., 2010; Corretti et al., 2014). The strategic location of Elba Island at the very cross-road of many trade routes through the Tyrrhenian Sea, and only a few miles distant from the Etruscan town of Populonia — one of the most important metalworking

centres of the whole Mediterranean region — greatly favoured a wide circulation of Elban iron in the Western Mediterranean since at least the 6th century BC (Corretti et al., 2014). According to Diodorus Siculus in the 1st century BC (but even earlier) a complex 'metallurgical chain' involved the working of iron well outside Elba Island, supporting a long-distance trade of iron (both as raw metal — blooms or bars — and ore) from the island (Diodorus, Bibliotheca Historica, liber V, 13). Therefore, retrieving the provenance of iron ore, bloom and/or semi-finished products would be of the utmost relevance for the reconstruction of ancient trade routes in the Mediterranean region. Recently, Benvenuti et al. (2013) proposed that the peculiar W-Sn signature of the hematite-rich ores from eastern Elba Island provides us with a powerful tool to ascertain the extent of trading of Elba's iron in the Mediterranean area in antiquity. As suggested by these authors, it would be very important to ascertain whether the characteristic W−Sn-rich geochemical signature of Elba iron ores is still detectable through the various steps of the *chaîne opératoire* of iron production, as apparently suggested by analyses of the bloom recovered at Baratti as well as of many smelting and smithing slags from Baratti and several

---

archaeological sites of Elba Island (Benvenuti et al., 2013). It becomes important, therefore, to evaluate how the mineralogical and chemical composition of iron ore, furnace materials (other than fluxes and charcoal) employed for the metallurgical process influence the trace element distribution (namely, W and Sn concentration) in the metallurgical products (slags and bloom). After the pioneering work by Hedges and Salter (1979), in the last fifteen yeas a large wealth of scientific papers have been devoted to iron provenancing in central and northern Europe (Buchwald and Wivel, 1998; Schwab et al., 2006; Dillmann and L'Héritier, 2007; Blakelock et al., 2009; Desaulty et al., 2008, 2009; Brauns et al., 2013; Charlton, 2015). To our knowledge, Sn was never investigated as a potential provenance tracer while tungsten was considered by Desaulty et al. (2009) only. This is apparently due, at least in part, to the different type of iron ores exploited in antiquity in the Tyrrhenian area (Elba island) with respect to central-northern continental Europe.

In this paper we report the first results of archaeometallurgical experiments performed both outdoor and in the laboratory primarily to investigate the extent of Sn and W partitioning during the various steps of the *chaîne opératoire* of bloomery iron production. As described in detail here below, the main target of our experiments was not to reproduce early processes of iron production carried out in ancient Etruria since the half of the 1st millennium BC but, rather, to compare the mineralogical, textural and chemical features of the bloomery products (namely, bloom and slag) with those found at archaeological sites. In particular, we wanted to test whether the peculiar geochemical features of hematite-rich iron ores from NE Elba, i.e., their co-enrichment in both W and Sn (Benvenuti et al., 2013) were still detectable in tapped slag and in the iron bloom. In parallel, in our lab investigations, we carried out several smelting experiments of a Sn/W-rich hematite ore from Elba (Terranera mine) under variable operating conditions (namely, temperature and oxygen fugacity) in order to evaluate the influence of these parameters on the final products (slag and metallic iron).

## 2. Etruscan iron smelting process: what we know

The furnace we built for our experiment was not modelled after any archaeological example, since at this preliminary stage of our research we were mainly interested in the smelting of a peculiar type of iron ore (W-Sn-rich hematite ore from eastern Elba mines: cf. Benvenuti et al., 2013) and the analysis of final products (bloom and slag) to ascertain the potential of geochemical markers (i.e., W and Sn contents) as tools for tracking provenance of ancient iron-made objects. On the other hand, notwithstanding metallurgical wastes related to ancient iron working are widespread both in Elba Island (cf. Corretti, 1988, 1991, with references) and southern Tuscany (Corretti and Benvenuti, 2001), archaeological evidence regarding bloomery furnaces of Etruscan to Roman age (8th—7th century BC up to 1st—2nd century AD) is scarce and partly unclear, thus actually hindering the reconstruction of a precise kind of smelting furnace.

Nevertheless, we have a rather defined idea of the general operation mode and the structure of an Etruscan smelting furnace. This awareness was obtained studying several iron working sites on the mainland such as Populonia (Benvenuti et al., 2000; with references), Follonica, Fonteblanda/Talamone and the Giglio Island to the south, Pisa and its harbours to the north, where iron exploited from Elban mines was worked between the 7th and the 5th century BC (Corretti et al., 2014; with references; see Fig. 1). As said above, however, the reported occurrences of "true" bloomery furnaces are only few and mostly from salvage excavations, which did not permit accurate description and analysis of the structures (Corretti and Benvenuti, 2001; Corretti et al., 2014). The earliest examples so far known of bloomery furnace in southern Tuscany were discovered in 1997 at Rondelli, near Follonica (Fig. 1), and were dated to 550—450 BCE according to Aranguren et al. (2004). They mostly appear to be open hollows in the ground lined with refractory clay, although it is not clear whether some kind of superstructure (shaft) was originally present and did not survive in the archaeological record (Aranguren and Paribeni Rovai, 1999). Salvage excavations in 1999 at the site of San Bennato, Cavo (northern Elba Island: Fig. 1) put to light archaeometallurgical remains which look very similar to the Rondelli site types and were dubiously interpreted as bloomery or forge furnaces of uncertain age (5th to 2nd century BC, Firmati et al., 2006). Recent studies of materials excavated at the archaeological site of San Giovanni (Portoferraio, Elba Island) led Manca et al. (2014) to advance the hypothesis that iron smelting in Roman times (3rd—1st century BC) was performed in furnaces made of refractory ceramics, and not armoured with stones.

Populonia, the Etruscan town built high on a promontory above the sea just in front of Elba Island (Fig. 1), after an earlier stage of copper production (Chiarantini et al., 2009b) became the major ironworking centre of Etruria probably since the 6th century BC and up to the 1st century AD (Corretti and Benvenuti, 2001). In the underlying Gulf of Baratti there is plenty of evidence of stone-made iron furnaces (although mostly as broken fragments). Here, a hypothetical iron smelting furnace was identified in 1977—1978 by M. Martelli and M. Cristofani during archaeological excavations in the metalworking area of Poggio della Porcareccia. The structure, archeologically dated to the 3rd century BC, was composed of blocks of a local beach sandstone ("Panchina"): it was cylindrical in shape and divided into chambers by a pierced slab supported by a clay pillar. However, according to Sperl (1985), given the inherent low thermal insulation, this structure was not suitable for smelting operations, but more likely it could have been used for the production of bricks or pottery. A second "furnace" identified by Voss (1988) inside a slag beach deposit (extending along the shoreline of the Baratti Gulf underneath the acropolis of Populonia) was cylindrical, with an inner diameter of 30 cm and about 45 cm high; the furnace wall was 15 cm thick and made of sandstone and clay that appeared intensively slagged. Voss suggested it was a non-tapping, smelting furnace and it was radiocarbon dated to 170 ± 70 BCE, i.e, to the Roman Republic period. A possible reconstruction of a "Baratti-type smelting furnace" has been proposed by Benvenuti et al. (2003) on the basis of furnace fragments from different places through the Baratti plain; in its general outline it consists of a low-shaft furnace of the slag-tapping type, with a shaft diameter not exceeding 40 cm. The common occurrence of tap holes/runners suggests that slags were tapped outside the furnace. Air was forced into the furnace by means of clay tuyères, probably equipped with bag bellows. Typical conical tuyères had a maximum internal diameter of about 8 cm and had circular or roughly square cross-sections. It is obviously difficult to establish the height above-ground of the furnace, but as deduced by the findings of furnace walls fragments, it possibly was not greater than about 1 m. Furnace walls were made of blocks of sandstone, commonly parallelepiped-shaped. This sandstone armour, several centimetres thick, was internally lined with clay. Benvenuti et al. (2003) suggest that the bottom of the furnace was made of a thin (3 cm thick on average) sandstone slate, also internally lined with clay. Subsequent findings after excavations on the Baratti slag beach deposit uncovered several smithing/reheating hearths employed for iron working and dated to the 5th—2nd century BC (Chiarantini et al., 2009a). These authors suggest that even Voss' furnace could be re-interpreted as a smithing hearth rather than a bloomery furnace.

From the brief review above outlined it comes out clearly that there is not a unique nor a specific type of Etruscan (or Roman) bloomery furnace in the area. Thus, since at this preliminary stage
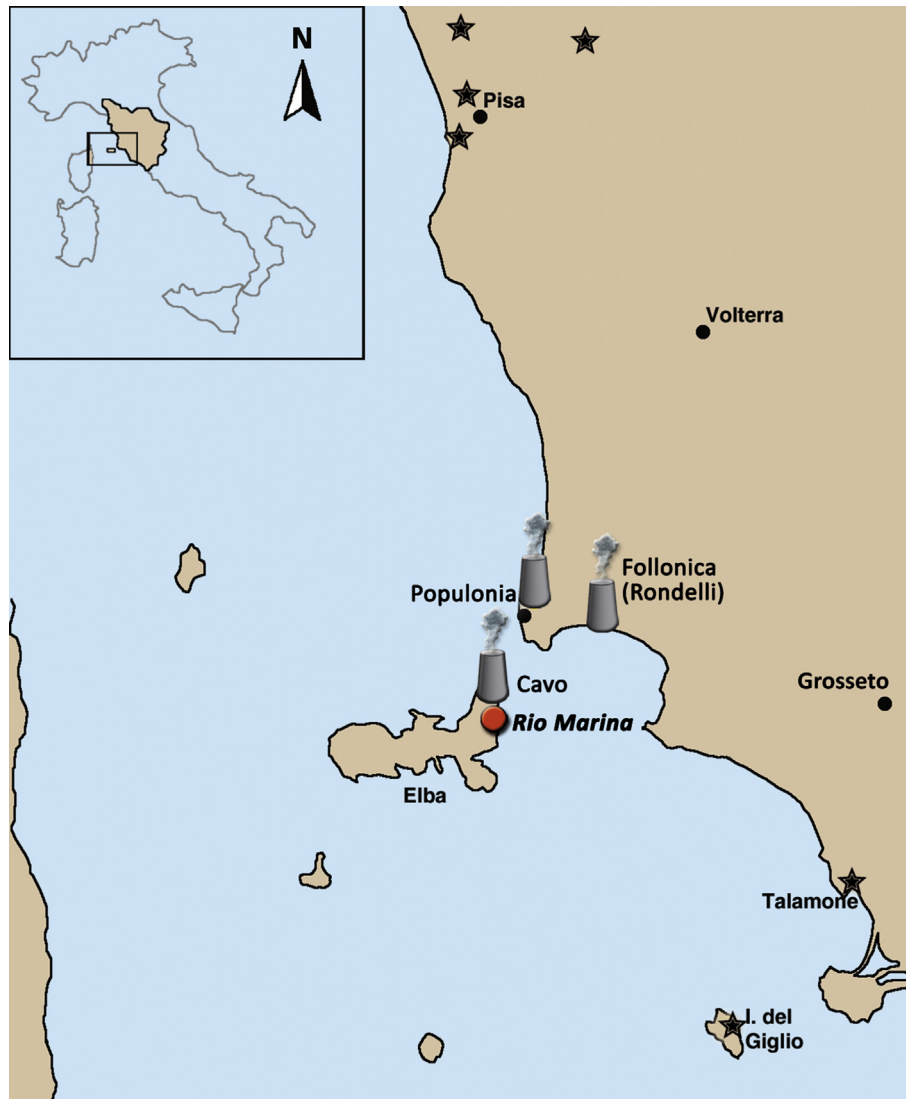
Fig. 1. Location of the sites mentioned in the text, including Rio Marina (Elba Island), where the outdoor experiment was carried out, and three major archaeometallurgical sites (marked by stylized furnaces) where remains of (presumed) smelting furnaces of Etruscan/Roman age have been reported. Black stars indicate sites where fragments of iron ore of presumed Elban provenance have been reported.

of our research we were mainly interested in smelting iron ore from Elba with peculiar geochemical features (i.e., showing Sn + W co-enrichment) and analysing the bloom and slag so far obtained, we decided to build a relatively simple shaft furnace made of local clay following the construction scheme provided by Sauder (2013), as illustrated in Section 4.1.

3. Analytical methods

Starting material (iron ore and clay from the Bacino/Rio Marina mine + commercial charcoal) and final products (slag, iron bloom) of the outdoor archaeometallurgical experiment were powdered (ore, clay, charcoal, slags) using an agate balls miller (adopting a rigorous cleaning procedure in order to avoid any contamination) and/or embedded in epoxy resin (Fe-rich ore, slags and bloom) in order to characterise their mineralogy, textural and compositional features. We selected for subsequent analysis a sample of iron ore as-mined that we deemed representative and, for a qualitative comparison, after roasting.

Major oxides and some trace elements were determined on

powders by XRF using a Rigaku-Primus II (Rh anticathode) at the CRIST laboratories (University of Firenze). Analyses were performed on compressed pellets. Quantitative analyses for major oxides were calibrated using international standards (Bauxite; IF-G) while trace elements have been analysed semi-quantitatively, due to the absence of international standards with suitable W and Sn concentrations. For this reason, in most samples, Sn and W concentrations have been determined using both XRF and ICP-MS data; the greatest discrepancies have been observed in slag samples where Sn was definitely overestimated using XRF (Table 2).

FeO contents were determined for iron ore and slags through titration with $K_2Cr_2O_7$ on acid digested samples following the "classic" method of Shapiro and Brannock (1962). LOI was determined by weighing powders before and after calcination at 950 °C; the obtained values were corrected for Fe oxidation assuming that Fe was fully oxidised after calcination.

ICP-MS analyses were performed on acid digested samples using a Perkin-Elmer NexION 300x instrument at the Dipartimento di Scienze della Terra (University of Pisa). All analytical details about acid digestion of samples (procedure and analytical grade of the

reagents) are provided in Benvenuti et al. (2013). A procedural blank was prepared along with each batch of samples and measurements (three replicates of 60 s for each sample) were corrected for blank subtraction, instrumental drift and isobaric interferences. The conversion from signal intensity to concentration was performed by external calibration, using the well-certified international geochemical reference sample BE-N, doped with known amounts of trace elements such as Sn and W (for further details about this procedure see Benvenuti et al. (2013). Detection limits for W and Sn are 0.2 and 0.4 $\mu g\ g^{-1}$, respectively. Analytical precision is generally better than 5% relative standard deviations for concentrations above 10 $\mu g\ g^{-1}$, and better than 10% for concentrations above 1 $\mu g\ g^{-1}$.

XRD spectra were acquired using a Philips PW1830 diffractometer (Dipartimento di Scienze della Terra, University of Firenze) equipped with a Cu anticathode operating at the scan speed of 1° 2θ per minute in the 5—70° range.

We performed EMP analyses (JXA-8600) at C.N.R.- Istituto di Geoscienze e Georisorse, U.O.S. (Firenze) using an accelerating voltage of 15 kV and a beam current of 10 nA. Data acquired were corrected using the PAP matrix correction. Particular care was taken in order to minimise the detection limits of Sn and W: the former was calibrated on a pure metal (Astimex 29) measuring the Lα line diffracted by a PET analysing crystal and operating counting times in samples of 60s on peak and 30s on each background position. Tungsten was calibrated on a pure metal (Astimex 34) using the Mα radiation, a TAP analysing crystal and the same counting times as for Sn. Under these conditions the detection limits − calculated considering the signal lying at a level 3σ above the mean background − are 0.08 wt% (Sn) and 0.05 wt% (W).

SEM-EDS analyses of an iron bloom (archaeological) sample from Baratti were carried out by a Zeiss EVO MA15 scanning electron microprobe at the Interdepartmental Centre for Electron Microscopy and Microanalyses (MEMA) of the University of Florence.

A set of experiments were performed using a Deltech gas-mixing vertical quench furnace (Model DT-31VT-OS2) at the Dipartimento di Scienze della Terra, University of Firenze. In this apparatus temperature is monitored and controlled by two B-type thermocouples and during the experimental runs it was increased at a 5 °C/min rate up to 1150 or 1200 °C. Such temperatures were selected because representative of prevailing conditions during the process of iron reduction in ancient bloomery furnaces, although higher temperatures could have been locally attained (cf. Pleiner, 2000; McDonnell, 2013). In addition, fO_2 control was achieved by continuously flowing an appropriate CO/CO_2 mixture through the furnace tube during the experiments. A sensor constituted by a solid zirconia ceramic electrochemical cell bonded to an alumina tube (SIRO2 oxygen sensor, Australian Oxytrol systems) allowed the direct measurement of both oxygen concentration and T (through an additional thermocouple) in the immediate vicinity of the experimental charges (about 2 cm above the sample container). Experimental runs were performed both in air and under reducing or highly reducing conditions ($CO/CO_2 = 5.6$—6.7 by volume) in order to ascertain the different phase assemblage formed in experimental products varying oxygen fugacity. The oxygen sensor recorded oxygen concentration generally was as constrained by the CO/CO_2 ratio of fluxed gas. Experimental charges were contained in platinum or ceramic crucibles and suspended in the hot spot of the furnace by means of a thin platinum wire connected to the thicker platinum quenching electrodes. At the end of the experiment, rapid quench was attained by melting the thin platinum wire via a current flow through electrodes; the sample dropped at the bottom of the furnace into a quenching pot filled with deionized water. In the experiments in which quenching was not performed the cooling rate was controlled at 5 °C/min. Duration of all the experimental runs was between 2 and 18 h.

4. Experimental reconstruction of a "bloomery" furnace

4.1. The 2013 outdoor experiment

From March 19 to 22, 2013, we conducted at Rio Marina mine (Elba Island: Fig. 1) an experimental reconstruction of a bloomery furnace entirely made of local clay. Our experiment was largely based upon Sauder's (2013) paper; both the construction of our furnace and the successful smelting of iron ore was made possible through a cooperation with Lucio Pari, an artistic blacksmith from Grosseto. The description of starting (clay, charcoal, iron ore, etc.) and final products of the experiment (slag, bloom) is reported in the following sections 4.2 and 4.3.

The preparation of the bloomery furnace required almost three days (19—21 March). About 70 kg of brownish-reddish clay from nearby outcrops of the Bacino open-pit mine (Fig. 2a) deriving from leaching and weathering of phyllitic formations of the Tuscan basement (Monticiano-Roccastrada Unit, Verruca and Rio Marina Formations: cf. Bortolotti et al., 2001; Pandeli et al., 2013), were taken and well-worked in order to obtain a relatively dry but still reasonably plastic consistency. We built a plinth for the furnace by setting eleven refractory bricks in a circular ring and filled the interstices among bricks with charcoal fines. Then we put on the plinth a wooden form 110 cm high, with a base diameter of 25 cm and top diameter of 16 cm (Fig. 2b). Lucio Pari (the blacksmith) built the shaft by adding lumps of clay in a spiral fashion around the form, with diminishing thickness of the clay wall moving from the base (about 6 cm) to the top (about 2 cm). After several hours of hard work, at 9:00 p.m. of the second day (March 19th) our clay furnace was ready (Fig. 2c). The furnace was left to air dry for the next 36 h and then fired lightly from the outside (Fig. 2d). We cut two holes, one in the front for tapping slag and one in the flank for the insertion of the tuyère (Fig. 2e). Subsequently we fired the wooden form up to complete combustion. We reinforced the top of the furnace by applying a girdle of hemp mixed with brick dust, clay and plaster. We cut a tuyère hole at a height of 30 cm from the furnace bottom purposed to accommodate a clay tuyère with an inner diameter of about 2 cm, angled downwards at approximately 17° (Fig. 2f).

A whole day (March 20) was necessary for sampling, beneficiation and roasting of hematite ± pyrite + quartz ore (Fig. 3a) taken from outcrops of the Bacino opencast mine at Rio Marina. We took about 110 kg of iron ore, less than half of which (about 45 kg) was used in our experiment. The iron ore was crushed and then roasted to increase porosity and/or friability by the removal of volatile gasses such as sulphur (Fig. 3b—c), in accordance with reports from the ancient geographer Diodorus, in fact, where Elban hematite ore is said to have been roasted on the Island "using a great fire and forming spongy conglomerates which were transported to the coast of the Etruscan mainland for conversion to iron" (Diodorus 5.13, as cited by Pleiner, 2000).

On the morning of Friday 22 March, we were finally able to start the smelting experiment (Table 1). We reshaped the tap arch in a rectangular form (approximately 9 cm wide and 30 cm high), and after preheating the furnace for almost an hour with a wood fire (introduced from the tap hole), we closed the tap hole and started burning charcoal with forced air fed through the tuyère by a compressor (380 V; blowing rates ≥50 L/min; see Table 1 and Fig. 2f). At 2:30 p.m. we started charging 1.5 kg of ore at the top of a charcoal-full furnace. Then we reduced the amount of ore for each charge to 750 g, maintaining a 1:1 ore to fuel weight ratio. The charges were introduced in the furnace's chimney approximately every 5 min for the whole duration of the smelting process (about

Fig. 2. Different steps in the construction of the clay furnace employed in the outdoor smelting experiment. (a) Outcrop of the clay-rich horizon in the Bacino open-pit mine from which clay was taken for the experiment; (b) Frontal view of the wooden form put on the plinth made of refractory bricks; (c) The air-dried clay furnace; (d) Firing of the furnace's external surface; (e) Cut of the frontal hole for slag tapping and of the lateral one for tuyère insertion; (f) The furnace immediately before the beginning of the smelting experiment.

6 h: Table 1). At 4:30 p.m. we opened the tap slot (Fig. 4a) and tapped out the first run slag (Fig. 4b—d), followed by four other runs. Each run slag was sampled for further analysis (see chapter 3.3). The 5th slag tapping and last (53rd) furnace charge were made at 7:00 p.m. From this time we stopped adding iron ore and we only charged the furnace with charcoal for almost 1 h. Then we opened the tap hole, broke the basal plinth and partial wrecked the front of the furnace to facilitate bloom removal (Fig. 5a). The bloom was recovered in three pieces of about 1.5 kg each, partially embedded in a solid, viscous slag (Fig. 5b). To be noticed that, after extraction of the bloom, it became evident that the furnace walls in correspondence of the location of the bloom were intensely reduced in thickness and clearly corroded due to reaction with liquid slag in the furnace (Fig. 5c). The bloom still hot was partially worked immediately after the withdrawal (Fig. 5d), although final forging was accomplished in the following days by the blacksmith Lucio Pari in his workshop at Grosseto. A summary of the amount of starting materials used for the experiment and of the final products is reported in Table 1.

4.2. Analysis of iron ore, clay and charcoal

Iron ore, clay and charcoal used in the outdoor archaeometallurgical experiment were characterized using XRD, XRF, ICP-MS, SEM and EMP (the latter only for iron ore). Particular attention was paid to the mineralogical speciation and concentrations of Sn and W in the analysed products. Results of bulk mineralogical (XRD) and compositional analyses (ICP-MS and XRF) are reported in Table 2.

Iron ore, sampled in the nearby Bacino open-pit mine,[1] was analysed before and after roasting just to investigate (in a qualitative way) the chemical and mineralogical modifications occurred during the experiment. As-mined ore is constituted mainly by hematite ± magnetite and euhedral pyrite in a silicate matrix (quartz, micas, clay minerals). Bulk contents of W and Sn of both as-mined and roasted ore are relatively high (around 650 ppm and 100 ppm, respectively: Table 2). However, only a tungsten phase (scheelite, $CaWO_4$) was observed in our samples, preferentially hosted within magnetite (BSE-EMP images: Fig. 6); neither cassiterite nor any other Sn phase was detected, unlike the case of the Terranera mine iron ores reported by Benvenuti et al. (2013).

However, we cannot exclude that unevenly distributed, small crystals of cassiterite may actually contribute to the observed bulk

---

[1] We used this kind of ore, although less (W + Sn)-rich than the massive hematite ore from Terranera mine employed for our indoor experiments (chapter 5), since the latter was not available in sufficient amount for the outdoor smelting experiment.

Fig. 3. (a) Run-of-mine iron ore (each ore fragment is approximately 10 cm large); (b) Ore crushing; (c) Roasting of iron ore to eliminate volatiles.

authors (e.g. Tarassov et al., 2002). Differently, W in magnetite and Sn in both hematite and magnetite are constantly below the detection limits. The major contribution to the relatively high LOI contents (4.2 wt %) of as-mined ore is likely provided by sulphur volatilisation after breakdown of pyrite to iron oxides (cf. Pleiner, 2000).

The clay used in the outdoor archaeometallurgical experiment, sampled in the Bacino open-pit mine, is principally made of clay minerals, iron hydroxides (goethite) and hematite associated with minor amounts of quartz, feldspars and talc (Table 2). In accordance with mineralogy, chemical analyses highlight a high iron content (above 40 wt% Fe_2O_3) and significant amounts of trace Sn and W (41 and 178 ppm, respectively; Table 2).

Charcoal used for the experiment was natural wood charcoal produced at Montorsaio, 20 km north of Grosseto in southern Tuscany (Lucio Pari, personal communication). After calcination at 950 °C in our lab (see Section 2) we obtained an ash residue (total ash) corresponding to about 4% of the mass of burned charcoal, which was then analysed by means of XRF. The blackish ash residue was largely constituted by Ca (more than 80 wt% CaO: Table 2) and minor amounts of Mg, S, P, K. Charcoal ashes showed significant Sn contents (268 ppm). If we consider that about 25 g of charcoal are necessary to obtain 1 g of ash after combustion (cf. Table 2), this datum would indicate a content of about 10 ppm Sn in the dry charcoal. This appears to be a not negligible contribution to the overall chemical budget of the smelting process, and should be taken in account in provenance studies (see discussion below).

4.3. Slag and bloom analysis

Samples of experimental products (slag and bloom) have been analysed for their chemical and mineralogical compositions (Table 2).

Five slag batches (samples S1 to S5) were tapped from the furnace after 1 h, 2 h, 2 h 45′, 3 h 15′ and 3 h 45′ from the beginning of the experiment. Together with the solid slag attached to the bloom (SBL) they were analysed for their chemical and mineralogical features (Table 2). Slags were mainly composed by FeO, Fe_2O_3, SiO_2, Al_2O_3 and CaO. The FeO/Fe_2O_3 ratio did not change significantly during the first three steps of tapping (3.6—5.1) but showed a rapid increase in the fourth (8.2) and, especially, in the

Table 1
Summary of the main steps followed during the outdoor smelting experiment and overall budget (by weight, kg) of materials used for (and produced after) the outdoor smelting experiment.

Operation type	Duration	Details
Furnace pre-heating	70′	- Wood (10′) and wood + charcoal (1 h) refurnishing - No induced draught
Furnace charging	5½ hours	- Induced draught (about 50 L/min) - n. 53 ore + charcoal charges (approximately 750 g of iron ore + 750 g charcoal)
Slag tapping	nd	- n. 5 runs of slag tapped out of the furnace
Charcoal charging	60′	- Charge of the furnace with charcoal only
Bloom extraction	45′	- Opening of the tap hole and partial wrecking of the furnace to facilitate bloom removal - Bloom (about 5 kg) withdrawal
Budget (total consumption or production)	Clay … 70 kg Hematite-rich ore … 45 kg Charcoal … 75 kg Slag … 30 kg Bloom … 5 kg	

tin contents of iron ore. To be noticed that EMP analyses performed in the present work on hematite from the Bacino iron ore indicate tungsten contents in the range of 0.1—0.5 wt% thus suggesting solid solution of this element in hematite, as already proposed by other

last one (22.4) denoting a rapid increase of reducing conditions in the final steps of the experiment. With respect to tapped slag, SBL (i.e., slag adhering to the bloom) is richer in SiO_2, Al_2O_3, MgO and K_2O (and poorer in FeO), similarly to what observed by Høst-

Table 2

Chemical and mineralogical features of starting materials (iron ore, clay, and charcoal) and final products (slag, bloom) of the archaeometallurgical experiment. Major element composition of starting products and slag were obtained by XRF, except for LOI and FeO (if analysed); bloom's major element composition is the average of ten spot EMP analyses. The Fe_2O_3 values of clay and charcoal ashes (marked by a star) refer to total iron contents. The LOI contents of run-of-mine iron ore (4.2 wt%) and charcoal ashes (3.5 wt%) are entirely due to sulphur volatilisation (i.e., SO_2). Trace element composition was achieved by ICP-MS, XRF (values among parentheses) and EMP (among square brackets: Sn and W contents of the bloom, average of ten spot analyses). In the "Mineralogy" section of the Table, minor phases are reported among brackets. Key to abbreviations: chl = chlorite group, cst = cassiterite, fa = fayalite, fd = K-feldspar, Fe = metallic iron, gt = goethite, hem = hematite, kln = kaolinite group, micas = K-micas, ilt = illite group, mnt = montmorillonite group, mag = magnetite, py = pyrite, qz = quartz, sch = scheelite, slg-incl = slag inclusions (in the bloom), tlc = talc, wü = wüstite; na = not analysed; bdl = below detection limit.

	Starting materials					Experimental products						Bloom
	Iron ore		Clay*		Charcoal ashes	Slag						
	Run-of-mine	Roasted	Outcrop	Furnace wall		S1	S2	S3	S4	S5	SBL	
Chemistry												
wt%												[EMP]
SiO_2	5.8	8.7	28.5	29.7	0.1	14.1	14.8	11.8	12.6	16.6	22.7	Si 0.01
TiO_2	0.0	0.0	0.5	0.61	na	0.2	0.2	0.1	0.1	0.2	0.4	Ti 0.02
Al_2O_3	3.8	2.0	12.2	11.7	0.1	4.9	5.7	4.9	4.1	5.8	9.0	Al bdl
FeO	4.0	4.3	na	na	na	58.3	60.9	61.0	69.1	67.3	54.1	Cr 0.02
Fe_2O_3	78.7	83.5	40.9*	45.3*	0.1*	15.8	12.0	16.9	8.4	3.0	5.0	Fe 100.70
MnO	0.0	0.0	0.1	0.1	0.1	0.1	0.1	0.1	0.1	0.1	0.1	Mn 0.05
MgO	2.7	0.8	5.4	4.8	3.9	1.8	2.0	1.5	1.8	2.2	3.3	Ca 0.02
CaO	0.0	0.1	0.1	2.9	84.9	3.3	2.7	2.4	2.2	2.5	1.6	Mg bdl
Na_2O	0.0	0.0	0.0	0.1	0.4	0.1	0.1	0.1	0.1	0.1	0.1	K 0.01
K_2O	0.5	0.3	1.6	2.0	2.5	1.1	1.2	0.9	0.9	1.2	2.3	
P_2O_5	0.0	0.0	0.1	0.1	3.7	0.2	0.2	0.1	0.1	0.1	0.1	
LOI	4.2	0.2	10.1	2.1	3.5	0.0	0.2	0.0	0.3	0.7	1.1	
Σ	99.8	99.9	99.6	99.4	99.2	99.8	99.9	99.8	99.9	99.8	99.7	Σ 100.83
ppm												
W	656 (630)	(695)	204 (178)	346		605 (911)	(843)	621 (927)	(827)	541 (901)	473 (713)	86 [bdl]
Sn	75 (99)	(150)	91 (41)	bdl	(268)	33 (bdl)	(bdl)	32 (bdl)	(bdl)	36 (bdl)	32 (bdl)	30 [bdl]
Rb	26	na	197 (101)	217		41	(83)	26	(bdl)	39	91	1
Sr	6	na	41 (33)	308	(3831)	106	(69)	75	(48)	75	73	6
Zr	3	na	172 (58)	187		45	(58)	16	(46)	37	68	1
Mo	bdl	na	(bdl)			bdl		bdl		bdl	bdl	4
Sb	3	na	(12)			2		3		3	5	16
Ba	61	na	210 (344)	291		129	(bdl)	257	(bdl)	257	31	18
Ce	2	na	(22)			9		12		8	15	<1
Pb	7	na	476 (295)	977		22	(bdl)	9	(bdl)	55	119	<1
Th	1	na	(13)			5		3		4	8	<1
U	<1	na	(3)			2		<1		2	3	bdl
V	12	na	(71)			38		34		41	59	1
Cr	5	na	94 (73)	202	(1594)	19	(bdl)	28	(100)	26	51	1
Co	44	na	bdl (55)	89		25	(bdl)	94	(bdl)	25	48	231
Ni	3	na	123 (66)	151	(94)	10	(bdl)	16	(bdl)	15	39	119
Cu	5	na	354 (190)	321	(415)	54	(119)	29	(152)	52	111	82
Zn	108	na	1223(886)	1295		125	(135)	149	(83)	254	439	28
W/Sn	8.7(6.4)	(4.6)	2.2 (4.3)			18.3		19.4		15.0	14.8	2.9
Mineralogy	hem mag py qz micas chl kln	hem mag qz	chl kln ilt mnt hem gt qz fd tlc	na		fa wü micas (Fe) (cst)	fa wü micas	fa wü (sch) (Fe)	fa wü	fa wü micas qz (sch)	fa wü micas qz fd	Fe slg-incl

Madsen and Buchwald (1999) and Blakelock et al. (2009) in comparable material. The main mineralogy of slags includes subhedral laths of fayalitic olivine intermingled with dendrites of wüstite; moreover, skeletal crystals of olivine and wüstite are also scattered in the glassy groundmass. Rare, micrometric iron sulphides are associated with sub-micrometric scheelite crystals and tiny droplets of metallic iron (Fig. 7). It is likely that the scheelite crystals (together with mica and quartz detected in S1, S5 and SBL) do represent relic phases from the smelting of iron ore. Only in sample S1 we could observe one tiny crystal of cassiterite. EMP analyses revealed that olivine is a Mg-bearing fayalite ($Fe_{1.70}Mg_{0.30}SiO_4$) and that the glassy groundmass is mainly constituted by SiO_2 (32.9 wt%), FeO (37.5 wt%), CaO (10.8 wt%), MgO (4.7 wt%) and K_2O (2.9 wt%). The constantly low contents (below detection limits) of Sn and W in all major metallurgical phases (fayalite, wüstite, glass) indicate that these elements are mostly concentrated in specific phases. The tungsten contents of tapped slags vary from 470 to 620 ppm and may be well explained by the common occurrence of sub-micrometric scheelite. ICP-MS analyses show low amounts of Sn

(31–36 ppm) in all slag samples, possibly due to the uneven and scarce occurrence of cassiterite (detected only in slag S1).

The bloom extracted at the end of the outdoor smelting experiment is made of massive metallic iron with relatively few pores and slag inclusions, consisting of fayalite + wüstite + glass (Fig. 8). On the other hand, bulk ICP-MS analyses of the bloom show significant contents of siderophile elements like Co and Ni (231 ppm and 119 ppm, respectively), whereas Sn and W concentrations are of the same order of magnitude (30 ppm and 86 ppm, respectively).

The compositional patterns of ore, clay, charcoal ash, slags and bloom can be better evaluated following Crew's (2000) method of representation of analytical data. Thus, we have plotted in Fig. 9 major elements (Fig. 9a) and trace elements (Fig. 9b) composition of investigated samples after normalisation to the mean ore composition (run-of-mine ore). The following observations can be made:

- slag content of lithophile elements like Si, Al and Zr (and also Pb, which, notwithstanding his chalcophile-siderophile affinity, has

Fig. 4. (a) Breaking the front of the furnace for slag tapping out of it; (b) and (c) The first slag tapping; (d) a piece of slag tapped during the experiment.

been observed to partition between metal and slag: cf. Brauns et al., 2013) are clearly influenced by clay (cf. Crew, 2000), with a more pronounced effect for slag attached to bloom (SBL) with respect to tapped slag S1-S5;

- charcoal ashes mainly influenced the alkaline (K, Na) and alkaline-earth elements (Ca, Sr) content of slags;
- in agreement with Senn et al.'s (2010) experimental data, the yielded metal (i.e., the metallic portion of the bloom) is enriched in Cu, Ni, Co and Sb, and depleted in lithophile elements, Zn (probably lost due to volatilisation), V and Cr;
- apparently, neither W nor Sn are partitioned into the metallic phase; slags, on the other hand show normalised values close to (but less than) 1 for W. To be noticed that we could observe one single crystal of scheelite in the polished section of the bloom, close to a slag inclusion, but no cassiterite (nor any other Sn-bearing phase) at all.

5. Experimental smelting in a vertical quench furnace

5.1. Selection of samples and operating parameters

Lab experiments were designed to perform smelting of Elban iron ore under controlled conditions (i.e., temperature and oxygen fugacity) in order to test the behaviour of some geochemical markers (notably: W and Sn) as to their partitioning in slags and iron bloom during the smelting process.

We selected a different kind of iron ore with respect to the outdoor experiment above described. In particular, we chose, for this experiment, a sample (TN11) of massive hematite ore from Terranera mine (Porto Azzurro, Elba Island: Fig. 1), which, according to Benvenuti et al.'s (2013) study, has the highest Sn (6715 ppm) content and the second highest W content (4950 ppm) among all

iron ores (Table 3). We mixed the iron ore with different proportions of a fluxing medium (CS, quartz-rich sand from Cavoli, Elba Island) and fuel (CT, Tuscan charcoal, different from that used for outdoor experiment). The major element composition and mineralogy (as inferred from XRD analysis) of these three constituents are reported in Table 3.

After some preliminary tests, we prepared three mixtures (called A, B and C) of iron ore, flux and charcoal in the following proportions (by weight):

(A) 1 : 0 : 1
(B) 5 : 1 : 6
(C) 5 : 1 : 60

As shown in Table 4, in all experimental runs (except EXP 116 and EXP119) redox conditions in the furnace (i.e., fO_2) have been externally constrained by regulating the CO/CO_2 ratio in the gaseous mixture by fluxing the furnace chamber. Thus, the addition of charcoal to the mixtures — in most of our experiments — can be deemed largely ineffective in controlling the redox atmosphere, and its principal aim was to reproduce more faithfully the operating conditions of ancient metallurgical processes. The experiment EXP101 — performed using mixture A (no flux added) — was designed as a pilot test to test the viability of Fe reduction in short times, whereas run EXP119 (with charcoal-rich mixture C) allowed us to estimate the time required to get to complete charcoal consumption. For all other experiments we used mixture B.

5.2. Results

With the exception of run EXP112, at the end of the experiments all the crucibles contained newly formed phases (like fayalite and

Fig. 5. (a) After breaking the basal plinth, the tap hole was opened and the front of the furnace partially wrecked to facilitate bloom removal; (b) Close-up view of one of the three pieces of iron bloom; (c) The furnace after smelting: note the intense thinning of the lower part due to reaction with the charge; (d) The bloom still hot was partially worked immediately after extraction from the furnace.

wüstite) associated with relic, unreacted charge materials (not reported in Table 4). Metallic iron was the only phase detected in the crucible at the end of experiment EXP112, while it did not form at all in three runs (EXP101, EXP102 and EXP118), reasonably because the redox conditions into the furnace were not adequately reducing. Run EXP116 (one of the two performed in air, with no CO/CO$_2$ gas flow), was unsuccessful: reagents (mixture B) were recovered almost unreacted in the crucible after final cooling. We carried out a second experiment with no gas flow (EXP119) and by using the charcoal-rich mixture C. Although burning of the abundant charcoal in the charge initially produced a reducing atmosphere (the oxygen sensor recorded fO_2 as low as 10^{-13} atm: Table 4), rapid fuel consumption after less than 2 h prevented to obtain metallic iron among the final products, which included magnetite together with (relic) hematite. Plotting the operating conditions of different runs in a temperature versus log fO_2 graph (Fig. 10), we can observe a good agreement between theoretical and experimental data. For comparison, we have also reported in this diagram several buffers of oxygen fugacity (WM: wüstite-magnetite; IW: iron-wüstite; QIF: quartz-iron-fayalite; CCO: C—CO—CO$_2$). To be noticed that the latter buffer (CCO) is of particular importance for iron ore reduction in presence of solid carbon (i.e. charcoal) during bloom formation. In the temperature range 1100—1200 °C the CCO buffer lies about two logarithmic units below the IW buffer

and 1—1.5 below QIF (Fig. 10). It may be envisaged that, in the presence of silicate phases (like fayalite) in order to obtain metallic iron the fO_2 should fall in the range delimited by QIF and CCO buffers. In particular, at temperatures comprised between 1100 and 1200 °C, fO_2 values of $10^{-13}/10^{-15}$ atm are necessary to produce metallic iron. Accordingly, only in EXP112 run we obtained metallic iron together with glass, but no fayalite. When present, metallic iron preferentially occurred either as isolated patches or along the borders of glass pockets.

EMP analyses were conducted on metallic iron from EXP112 in order to test if — and to what extent — Sn and W have partitioned in solid iron during the smelting process. Results show that tin is present in significant amounts (0.21—0.30 wt% Sn), whereas tungsten is always below the detection limit (0.05 wt%). In addition EMP analyses show only trace contents (close or below detection limits) of Si, Ti, Al, Cr, Mn, Ca and Mg.

6. General discussion and conclusions

6.1. The experimental reproduction of iron smelting

6.1.1. Outdoor experiment (Rio Marina)

In the experiment performed at Rio Marina on March 2013 we succeeded in smelting iron ore from the nearby Bacino open-pit
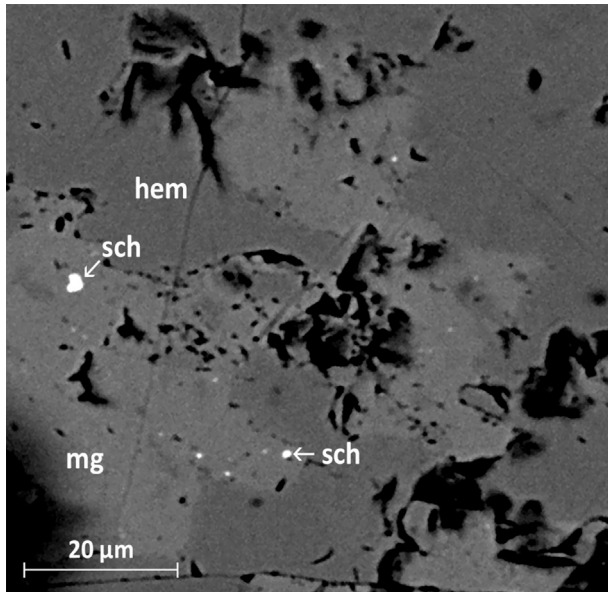
Fig. 6. BSE-EMP image of a representative sample of iron ore taken from the Bacino open-pit mine, used in the outdoor archaeometallurgical experiment. Legend: hem = hematite, mag = magnetite, sch = scheelite.
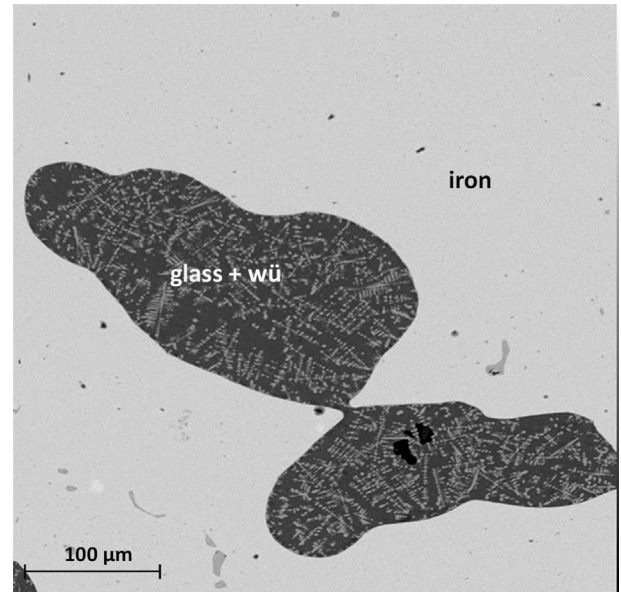

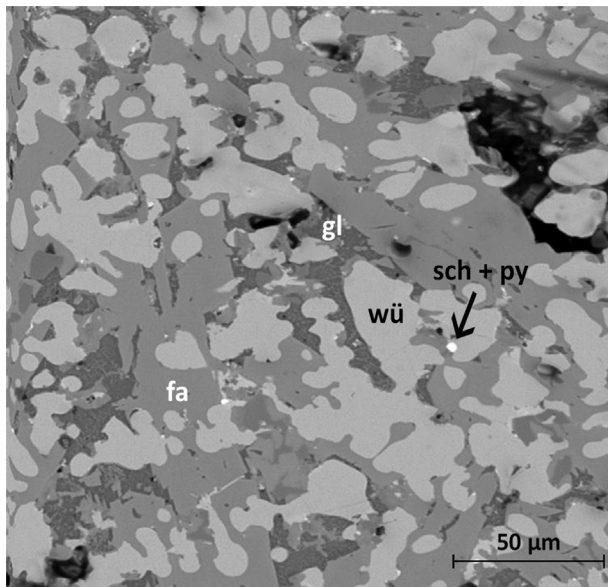**Fig. 8.** Electron backscattered image of the bloom produced at the end of the outdoor experiment. Legend: wü = wüstite.

Fig. 7. BSE image of tapped slag S5. Dendrites of wüstite (wü) and subhedral fayalite (fa) crystals are dominant. Small dendrites of wüstite are also scattered in the glassy groundmass (gl). Rare scheelite (sch) crystals are associated with sub-micrometric iron sulphides (py).
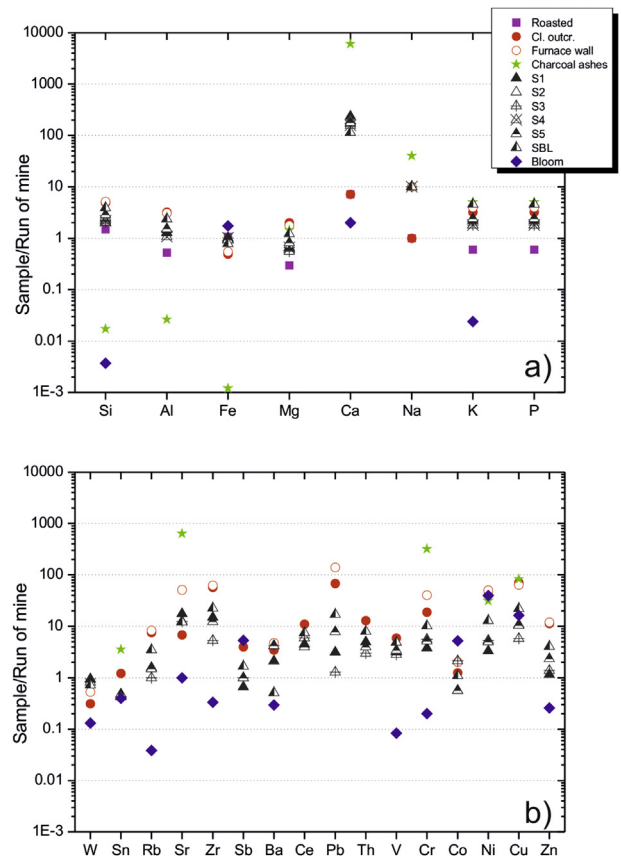

Fig. 9. Major elements (a) and selected trace elements (b), normalized to run-of-mine ore. Values (ICP data from Table 2) are reported in log scale.

mine at Rio Marina in a furnace entirely made of local clay (Mazzotta, 2014). Smelted ore consisted of massive hematite (±magnetite, pyrite) in a silicate matrix of quartz, micas, and clay minerals. The whole smelting process was characterized by maintaining a 1:1 ore to fuel ratio, without using any flux. Thus the iron ore proved to be substantially self-fluxing, although a significant contribution to the overall chemical budget of slags came from furnace walls, which appeared to be severely corroded and reduced in thickness at the end of the operations, and charcoal ashes (see Fig. 9 and discussion above). This clearly points to a limited refractoriness of the furnace, which was made of raw, untempered

clay well-worked in order to obtain a relatively dry but still reasonably plastic consistency. Notwithstanding this, shrinking and cracking of the furnace were neither extensive nor pervasive, and we could easily seal cracks (mostly developed in the upper part of
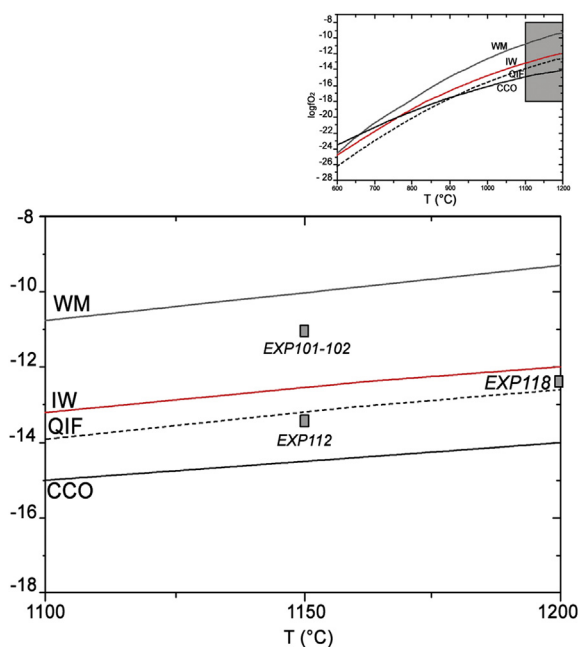
Table 3
Chemical and mineralogical features of iron ore, sand and charcoal used for the laboratory (indoor) experiment. All data have been obtained by XRF analyses, except for Sn and W contents of sample TN11 (ICP-MS, from Benvenuti et al., 2013). *calcined at 950 °C. Key to abbreviations: hem = hematite, qz = quartz, ab = albite, fd = K-feldspar, ms = muscovite (see also Table 2).

Major elements (wt%)	Iron ore (TN11)	Cavoli sand (CS)	Tuscan charcoal (TC)*
SiO_2	1.93	77.79	0.19
TiO_2	0.03	0.08	bdl
Al_2O_3	0.45	11.68	bdl
Fe_2O_3	96.05	0.48	bdl
FeO	0.44	bdl	bdl
MnO	bdl	0.01	bdl
MgO	0.12	0.65	7.54
CaO	0.03	1.34	85.39
Na_2O	0.17	2.66	0.38
K_2O	0.08	4.81	2.96
P_2O_5	0.01	0.02	3.28
LOI	0.69	0.48	bdl
Trace elements (ppm)			
W	4950	bdl	na
Sn	6715	bdl	na
Main mineralogy (XRD)			
	hem	qz ab fd ms	

Table 4
Operating conditions and final products of experimental runs. Neo-formed phases were detected by XRD. Glass is likely present in all experiments. Mineral abbreviations as in Table 2; ccm = cubic centimeters per minute. In EXP101 and EXP102 runs a Pt crucible was used and quenching took place at the end of experiments. In all other experiments a ceramic crucible was used and final products were slowly cooled (cooling rate: 5 °C/minute) down to ambient temperature.

	EXP101	EXP102	EXP112	EXP116	EXP118	EXP119
Mixture type	A	B	B	B	B	C
Charcoal/(sand + ore) (by wt)	1	1	1	1	1	10
Flux (granitic sand) addition	no	yes	yes	yes	yes	yes
T(°C)	1150	1150	1150	1200	1200	1200
duration (h)	2	2	2	18	2	2
CO (ccm)	9	9	10	no	10	no
CO_2 (ccm)	18	18	1.5	no	1.8	no
CO/CO_2	0.5	0.5	6.7	–	5.6	–
$logfO_2$ (atm)	−11.1	−11.1	−13.4	–	−12.5	<−13
"Metallurgical" products	wü	fa	Fe; glass	–	wü; fa	mt

Fig. 10. T-log fO_2 conditions imposed in experiments (squares). Wüstite-Magnetite (WM), Iron-Wüstite (IW), Quartz-Iron-Fayalite (QIF), C–CO–CO_2 (CCO) buffers are reported for comparison. In the presence of silicate phases, metallic iron is stable in the area delimited by CCO and QIF buffers.

the furnace) with fresh clay mixed with gypsum and brick powder. Liquid slag was tapped in five steps. Slags resemble in their mineralogical and textural features to analogue materials found at ancient ironworking sites, as for instance Baratti-Populonia, the most important site in ancient Italy for iron production during the Etruscan and Roman periods. The experiment was substantially successful, in that it allowed us not only to verify extent and mode of partitioning of geochemical markers like W and Sn into tapped slags and iron bloom (discussed below), but also to become more acquainted with the whole bloomery process in the light of future new experiments.

6.1.2. Indoor experiment (vertical quench furnace)

The "laboratory approach" to experimental smelting of iron ore through the utilization of a gas mixing furnace proved to be a useful and viable method to investigate the influence of physicochemical parameters such as T and fO_2 to the formation of silicate slag and metallic iron and the partitioning of geochemical markers (Sn and W) from the ore to the final products (slag and bloom). Nevertheless, it should be denoted that in this kind of experiments results are obtained under steady states thermodynamic conditions, which clearly differ from the multiple and simultaneous dynamic states characterizing a "true" bloomery process.

For our experiments we employed an iron ore (from Terranera mine) more than one order of magnitude richer in both Sn and W than the massive hematite ore from Bacino open-pit mine used for the outdoor experiment above described (Lazzeri, 2013). Given the scarcity of silicates in the ore charge, we added a sandy flux in

variable proportions, but with constant 1:1 (ore + flux)/fuel ratio. In the set of experimental conditions used for different runs (Table 4), however, we did never obtain the "typical" assemblage Fe (metallic iron) + fayalite + wüstite + glass usually found in "archaeological samples" and observed in slags produced with the outdoor experiment. This was probably due to the difficulty in reproducing in the lab experiments the fO_2 gradients which are expected to occur in bloomery furnaces. In fact, in our experiments with vertical quench furnace fO_2 is strictly controlled around the samples and gradients of this variable are negligible. Laboratory experiments have shown that metallic iron can be obtained in short times (2 h) at high T if log fO_2 is within QIF and CCO buffers. At more oxidizing conditions fayalite and wüstite are the only neo-formed phases whereas under more reducing conditions graphite may precipitate.

6.2. Behaviour of W and Sn

Table 5 summarizes the results obtained with our experiments concerning the partitioning of Sn and W in final products of iron smelting (slag and bloom/metallic iron). To be noticed that, for outdoor and lab experiments, we used iron ore from two different Elban mines (respectively, from Bacino/Rio Marina and Terranera mines). Given the similar geological framework and ore-forming environment (cf. Tanelli et al., 2001; Pandeli et al., 2013), in both cases the ore is constituted by a hematite + quartz ± pyrite assemblage. However, the Sn and W contents of the Terranera sample (6715 ppm and 4950 ppm, respectively) are noticeably greater than at Bacino (650 ppm and 100 ppm). Tungsten is apparently present both as mineral of its own (micrometric scheelite and/or ferberite crystals) and through solid solution in hematite. Cassiterite is present at Terranera mine (and specifically in sample TN11 used for indoor experiment) and is very likely the main Sn-carrier in Elban iron ores (cf. also Dunkel, 2002), although it has not been observed in our sample from Bacino/Rio Marina mine. As shown in Table 5, archaeological samples of iron ore found at S. Giovanni (a Roman iron-smelting site near Portoferraio, Elba island: cf. Alderighi et al., 2013; Manca et al., 2014) and Baratti-Populonia (Rescic, 1998) show a W/Sn ratio between 3 and 5, higher than at Terranera but smaller than at Bacino Mine.

In the overall, chemical budget of the outdoor experiment the role played by clay and charcoal ashes cannot be neglected, as shown in Fig. 9 and discussed above. The raw clay used in our outdoor experiment, taken from the Bacino open pit mine and largely formed after leaching and weathering of phyllitic host rocks of the iron ores, also showed significant W (178 ppm) and Sn (41 ppm) contents. Surprisingly, the charcoal employed for the same smelting experiment (commercial charcoal produced in the nearby of Grosseto, southern Tuscany) also have detectable contents of Sn (around 10 ppm), but not W.

As shown in Table 5, slag tapped from the Rio Marina smelting furnace shows the highest W/Sn ratio (15−19) when compared with iron ore (≈9) and the bloom (≈3). The occurrence of (relic?) scheelite and cassiterite − whose refractory behaviour is well-known − in some slag samples could indicate that the two elements are mostly transferred to the silicate melt as unreacted or partially reacted phases from the furnace charge. This could explain the somehow variable and unpredictable content of the two elements in the slaggy material due to a sort of "nugget-effect".

The metallic portion of the iron bloom produced in the Rio Marina experiment showed low amounts of W and Sn (86 and 30 ppm, respectively). On the other hand, one rare, tiny crystal of scheelite was observed within a slag, constituted by fayalite + wüstite + glass, included in the bloom. Spot EMP analyses of the metallic iron patches in the crucible at the end of EXP112 run showed high Sn contents (up to about 3000 ppm Sn), while W was constantly below detection limits (i.e., <500 ppm). The refractory behaviour of W-phases like scheelite and ferberite (the main tungsten-carriers in the Terranera iron ore used for the indoor experiment), which could have not (or only partially) reacted with other components in the crucibles, could explain the apparent "disappearance" of tungsten in the analysed final products (metallic iron) of EXP112 run. Alternatively, tungsten could have partially partitioned into the glass, which, due to its scarcity, could not be analysed.

It is interesting to make a comparison between the products (slag, bloom) which we have obtained in our outdoor experiment with "archaeological" analogues found at Populonia-Baratti in previous studies (Rescic, 1998; Strillozzi, 1998; Benvenuti et al., 2000, 2013; Chiarantini et al., 2009a). Tapped slags from various sites in the Baratti plain show extremely variable Sn contents, from below detection limit (around 5 ppm) up to thousands of ppm (3760 ppm of C6-47/4 sample, Campo VI site: Mariani, 2000), mostly between 50 and 150 ppm (Benvenuti et al., 2000). The latter authors described the occurrence of micrometric globules of iron-tin alloys (around 5 μm in size) approximating to FeSn and FeSn$_2$ in composition (quantitative SEM-EDS analyses), mostly disseminated in the glassy groundmass of iron slags. Although they did not

Table 5
Summary of the mineralogical and chemical speciation of tungsten and tin in iron ores, slag and bloom/metallic Fe. Except for the bloom produced with the indoor experiment (EMP spot analyses), all other analytical data have been obtained by XRF or ICP-MS techniques. Data from: Rescic (1998), Strillozzi (1998), Benvenuti et al. (2000, 2013), Mariani (2000), Chiarantini et al. (2009a). For Terranera Mine, in addition to the W and Sn content of the TN11 sample (used in our indoor experiment), we have also indicated among square brackets the overall compositional variation (from Benvenuti et al., 2013).

Provenance of ore/Location of the archaeological site	Tracers	ORE			SLAG			BLOOM		
		Mineralogical speciation	Contents (ppm)	W/Sn	Mineralogical speciation	Contents (ppm)	W/Sn	Mineralogical speciation	Contents (ppm)	W/Sn
Outdoor smelting experiment (clay furnace)	W	W-rich hem; sch	656	≈9	sch	473−621	15−19	sch?	86	≈3
Bacino (Rio Marina) Mine	Sn	cst?	75		cst	32−36		?	30	
Indoor experiment (vertical quench furnace)	W	sch; frb	4950 [19−4950]	0.7 (0.1−0.9)	-	-		?	<500	<0.2
Terranera Mine	Sn	cst	6715 [26−7828]		-	-		?	3000−2100	
Archaeological samples	W	sch; frb	63−2200	≈4−5	sch; frb	344−1958	10−21	-	-	
S. Giovanni (Portoferraio)	Sn	cst	34−466		?	34−189		-	-	
Baratti-Populonia	W	sch	1803	3	sch	944−1509	≈10−11	sch	865	1.8
	Sn	cst	<20−670		FeSn, FeSn$_2$	5−3760		Sn in metallic Fe	480	

analyse the bulk tungsten content of slags, nevertheless they evidenced the common occurrence of relic scheelite (particularly in the "Industrial Quarters" site). In addition, Strillozzi (1998) found an unusual W-enrichment of the glassy groundmass in a few samples (up to about 0.7 wt% W, EDS semi-quantitative analyses). New analyses of Baratti iron slags were recently provided by Benvenuti et al. (2013). Results indicate higher absolute concentrations of both W and Sn with respect to our "experimental" samples, but slightly lower W/Sn ratios (around 10—11: see Table 5). Slag adhering to a fragment of "proto-bloom" showed an even lower W/Sn ratio (4.1), but higher than the "proto-bloom" itself (1.8). For the present work we have analysed (by EMP) this sample in more detail and we could observe that the metal does contain systematically about 100—200 ppm Sn, and that abundant, partially reacted scheelite crystals occur within the glassy and slagged portions of the bloom (Fig. 11).

The behaviour of tungsten and tin during iron smelting operations has been so far little investigated, probably because these two elements are not typically enriched in the most common types of iron ore of central-northern Europe which were smelted in antiquity (including bog iron, oolitic and sideritic ores: Buchwald and Wivel, 1998; Schwab et al., 2006; Desaulty et al., 2009; Leroy et al., 2012). Actually, Desaulty et al. (2009) analysed the tungsten (but not tin) content of slag and ores from Pays de Bray, France, and concluded that this element (together with Mo) has "a more surprising behaviour or one that can vary depending on the experiment". Senn et al. (2010) used for their experimental bloomery smelts the hematite ore from Gonzen Mountains (Wolfslochstollen, Switzerland), which show some resemblance with hematite ores from Elba island; unfortunately, they analysed only a limited set of trace elements (including Sr, Ba and V). In their pioneering work on source determination of iron artefacts, Hedges and Salter (1979) compared the major and trace element composition of slag inclusions in currency bars with likely iron sources from southern England, including "nodular" ores (including sideritic and limonitic ironstones: cf. Paynter, 2006) and hematite ores. But, once again, neither tungsten nor tin were taken into consideration in this study. Therefore, a comparison with results obtained by other authors seems at this stage impossible.

We can stress that in our experimental (indoor and outdoor) bloomery processes that employed hematite ores with pronounced geochemical anomalies in W and Sn, the ratio between the two elements tends to increase passing from ore to slag, and to decrease

from ore (and slag, of course) to the bloom (see Table 5). A similar trend is followed by trace elements of ancient ore charges, slag and "proto-bloom" from Baratti and S. Giovanni archaeological sites, although we have not clear-cut evidence that metallurgical products (ie, slag and bloom) are coeval.

In most cases, our results indicate that the preferential partitioning of tungsten with respect to tin in the silicate slag is mostly linked to the persistence of (relic?) W-phases of their own in slags (scheelite, ferberite), although the glassy groundmass of some iron slags from Baratti may show appreciable enrichment in tungsten (Strillozzi, 1998). Tin, on the other hand, apparently shows a more siderophile behaviour than tungsten, and it can dissolve significantly in the metallic phase (up to about 3000 ppm: Table 5).
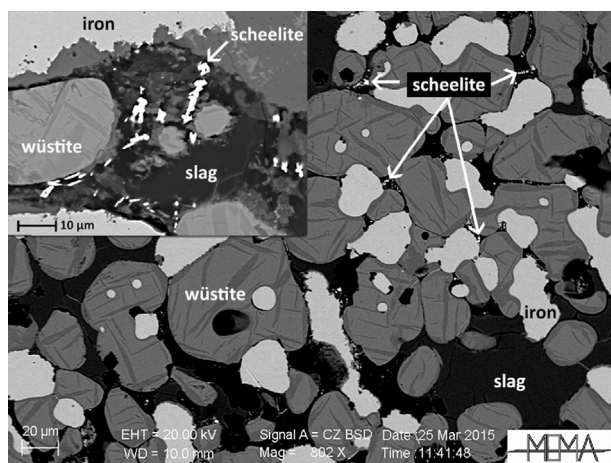
6.3. Conclusions

In this study we have tried to reproduce ancient bloomery processes used in Tuscany in Etruscan-Roman period, with the main goal to ascertain the behaviour of two chemical elements, W and Sn, which in a previous study (Benvenuti et al., 2013) were indicated as promising new provenance tracers for ironworking activities connected with the use of the massive hematite ores of Elba island. We adopted two different experimental strategies, including an outdoor experimental reproduction of iron smelting in a clay furnace and a laboratory test by means of a vertical quench furnace.

The experiments allowed us to verify that, depending on operating conditions, tin can significantly partition into the metallic iron phase (in the order of about 50% of the original content in the iron ore), whereas tungsten is predominantly transferred into the silicate slag, mostly (?) as relic, unreacted scheelite. These experimental results are substantially in agreement with observations made on "archaeological" samples (slag, bloom) found in two Etruscan/Roman iron-working sites (S. Giovanni and Baratti-Populonia) where iron was obtained from smelting of W- and Sn-rich hematite ore (Benvenuti et al., 2000, 2013). The recovery of "hardhead" phases (iron-tin alloys, approaching FeSn and Fe_2Sn in composition) in some slag from the Industrial Quarters area at Baratti (Benvenuti et al., 2000) provides further evidence for the strong affinity of tin with iron.

We conclude that a careful mineralogical, textural and compositional (bulk and mineral chemistry) analysis of slags produced by smelting of W-Sn-rich hematite ores like those occurring in the eastern portion of Elba island should permit to detect the presence of these elements in phases of their own, either relic (scheelite, ferberite, cassiterite) and/or newly formed (iron-tin alloys). Iron bloom obtained from this kind of iron ore could also bear evidence of the peculiar geochemistry of smelted ore, with tungsten preferentially associated with slag inclusions and tin eventually enriched in the metallic phase.

Acknowledgments

Fig. 11. BSE image of Baratti iron bloom, showing dendrites of wüstite and metallic iron with minor silicate slag. Abundant crystals of partially reacted scheelite are observable within the silicate slag-rich portions.

SEM analyses at MEMA (University of Firenze). Financial and logistic support for our outdoor experiment at Rio Marina was kindly provided by the Mining Park of Rio Marina (now Mining Park of Elba Island). The laboratory experiment benefitted from a MIUR (PRIN 2010-11, responsible P. Costagliola) grant. We also acknowledge the financial support provided by Ente Cassa di Risparmio di Firenze for implementation of the SEM and EPMA instrumental facilities used for this work. Finally, our thanks go to the two anonymous referees for all their helpful suggestions and comments on the first draft of this paper and to Marcos Martinón-Torres for editorial handling and stylistic revision of the manuscript.

References

Alderighi, L., Benvenuti, M., Cambi, F., Chiarantini, L., Chiesa, X.H., C., Corretti, A., Dini, A., Firmati, M., Pagliantini, L., Principe, C., Quaglia, L., Zito, L., 2013. Aithale. Ricerche e scavi all'isola d'Elba. Produzione siderurgica e territorio insulare nell'antichità. Suppl. Agli Ann. della Scuola Norm. Super. Pisa Cl. Lett. Filos. 5 (2), 169–188.

Aranguren, B.M., Ciampoltrini, G., Cortesi, L., Firmati, M., Giachi, G., Pallecchi, P., Rendini, P., Tesi, P., 2004. Attività metallurgica negli insediamenti costieri dell'Etruria centrale fra VI e V secolo a.C. In: Lehoërff, A. (Ed.), L'artisanat métallurgique dans les sociétés anciennes en Méditerranée occidentale, Proceedings of conference Ravello 2000, Rome (Italy), pp. 323–339.

Aranguren, B.M., Paribeni Rovai, E. (Eds.), 1999. Follonica etrusca: i segni di una civiltà. Panels of the exhibition Follonica, Florence (Italy).

Benvenuti, M., Chiarantini, L., Norfini, L., Casini, A., Guideri, S., Tanelli, G., 2003. The "Etruscan tin": a preliminary contribution from researches at Monte Valerio and Baratti-Populonia (southern Tuscany, Italy). In: Giumlia-Mair, A., Lo Schiavo, F. (Eds.), The Problem of Early Tin, Acts of the XIV UISPP Congress, University of Liège (Belgium), 2-8 September 2001, BAR Int. Series 1199, pp. 55–65.

Benvenuti, M., Corretti, A., Giardino, C., 2010. Iron and change in Europe – the first 2000 years. A contribution from Italy. In: Scientific Report of ESF SCH Exploratory Workshop, March 27–28, London (UK).

Benvenuti, M., Dini, A., D'Orazio, M., Chiarantini, L., Corretti, A., Costagliola, P., 2013. The tungsten and tin signature of iron ores from Elba Island (Italy): a tool for provenance studies of iron production in the Mediterranean region. Archaeometry 55, 479–506.

Benvenuti, M., Mascaro, I., Costagliola, P., Tanelli, G., Romualdi, A., 2000. Iron, copper and tin at Baratti (Populonia): smelting processes and metal provenances. Hist. Metall. 34, 67–76.

Blakelock, E., Martinón-Torres, M., Veldhuijzen, H.A., Young, T., 2009. Slag inclusions in iron objects and the quest for provenance: an experiment and a case study. J. Archaeol. Sci. 36, 1745–2157.

Bortolotti, V., Fazzuoli, M., Pandeli, E., Principi, G., Babbini, A., Corti, S., 2001. Geology of central and eastern Elba island. Ofioliti 26, 97–150.

Brauns, M., Schwab, R., Gassmann, G., Wieland, G., Pernicka, E., 2013. Provenance of iron age iron in southern Germany: a new approach. J. Archaeol. Sci. 40, 841–849.

Buchwald, V.F., Wivel, H., 1998. Slag analysis as a method for the characterization and provenancing of ancient iron objects. Mater. Charact. 40, 73–96.

Charlton, M.F., 2015. The last frontier in 'sourcing': the hopes, constraints and future for iron provenance research. J. Archaeol. Sci. 56, 210–220.

Chiarantini, L., Benvenuti, M., Costagliola, P., Cartocci, A., Fedi, M.E., Guideri, S., 2009a. Iron production in the Etruscan site of Populonia: new data. In: Nicodemi, W. (Ed.), Selected Papers of 2nd International Conference, Archaeometallurgy in Europe 2007, June 17-21 2007. AIM, Milano, pp. 221–231.

Chiarantini, L., Benvenuti, M., Costagliola, P., Fedi, M.E., Guideri, S., Romualdi, A., 2009b. Copper production at Baratti (Populonia, southern Tuscany) in the early-Etruscan period (IX-VIII cent. BC). J. Archaeol. Sci. 36, 1626–1636.

Corretti, A., 1988. Indagine preliminare sull'attività di riduzione del ferro in età romana all'isola d'Elba. Geo-Archeologia 7–39.

Corretti, A., 1991. Metallurgia Medievale All'Isola D'Elba. Edizioni All'Insegna del Giglio, Florence.

Corretti, A., Benvenuti, M., 2001. The beginning of iron metallurgy in Tuscany; with special reference to Etruria Mineraria. Mediterr. Archaeol. 14, 127–145.

Corretti, A., Chiarantini, L., Benvenuti, M., Cambi, F., 2014. The Aithale project: men, earth and sea in the Tuscan Archipelago (Italy) in antiquity. Perspectives, aims and first results. In: Cech, B., Rehren, T. (Eds.), Early Iron in Europe, Instrumentum Monographies 50. Édition Monique Mergoil, Montagnac, pp. 181–196.

Crew, P., 2000. The influence of clay and charcoal ash on bloomery slags. In: Tizzoni, C.C., Tizzoni, M. (Eds.), Iron in the Alps: Deposits, Mines and Metallurgy

from Antiquity to the XVI Century. Bienno: Proceedings of the International Conference (October 2-4, 1998), pp. 38–48.

Desaulty, A.M., Mariet, C., Dillmann, P., Joron, J.L., Fluzin, P., 2008. A provenance study of iron archaeological artefacts by inductively coupled plasma-mass spectrometry multi-elemental analysis. Spectrochim. Acta Part B 63, 1253–1262.

Desaulty, A.M., Dillmann, P., L'Héritier, M., Mariet, C., Gratuze, B., Joron, J.L., Fluzin, P., 2009. Does it come from the Pays de Bray? Examination of an origin hypothesis for the ferrous reinforcements used in French medieval churches using major and trace element analyses. J. Archaeol. Sci. 36, 2445–2462.

Dillmann, P., L'Héritier, M., 2007. Slag inclusion analyses for studying ferrous alloys employed in French medieval buildings: supply of materials and diffusion of smelting processes. J. Archaeol. Sci. 34, 1810–1823.

Dünkel, I., 2002. The Genesis of East Elba Iron Ore Deposits and Their Interrelation with Messinian Tectonics, Tuebinger Geowiss. Arb., Reihe A 65. Publication Geological and Paleontological Institute, University of Tuebingen.

Firmati, M., Principe, C., Arrighi, S., 2006. L'impianto metallurgico tardo repubblicano di San Bennato all'Isola d'Elba. ΑΓΩΓΗ 3, 306–312.

Hedges, R.E.M., Salter, C.J., 1979. Source determination of iron currency bars through analysis of the slag inclusions. Archaeometry 21, 161–175.

Høst-Madsen, L., Buchwald, V.F., 1999. The characterization and provenancing of ore, slag, and iron from the iron age settlements at Snorup. Hist. Metall. 33, 57–67.

Lazzeri, L., 2013. Studi in Archeometallurgia Sperimentale per la Riproduzione dei Processi Antichi della Produzione del Ferro. Unpublished thesis. University of Florence.

Leroy, S., Cohen, S.X., Verna, C., Gratuze, B., Téreygeol, F., Fluzin, P., Bertrand, L., Dillmann, P., 2012. The medieval iron market in Ariège (France). Multidisciplinary analytical approach and multivariate analyses. J. Archaeol. Sci. 39, 1080–1093.

McDonnell, G., 2013. Temperature profiles and cast iron production in experimental iron smelting furnaces. Hist. Metallurgy Soc. Occas. Publ. 7, 61–68.

Manca, R., Pecchioni, E., Benvenuti, M., Cambi, F., Chiarantini, L., Corretti, A., Costagliola, P., Pagliantini, L., 2014. Archaeometric study of ceramic materials from archaeological excavations at the Roman iron-working site of san Giovanni (Portoferraio, Elba island). Proceedings of SGI-SIMP congress, september 10-12, milan (Italy). Rendiconti Online della Soc. Geol. Ital. 31 (Suppl. 1), 265.

Mariani, A., 2000. Studio Archeometallurgico di Resti dei Forni Siderurgici Etruschi Provenienti dai Quartieri Industriali di Baratti (Populonia). Unpublished thesis. University of Florence.

Mazzotta, C., 2014. La Tracciabilità del Ferro Elbano: uno Studio di Archeologia Sperimentale e di Archeometallurgia. Unpublished thesis. University of Florence.

Pandeli, E., Principi, G., Bortolotti, V., Benvenuti, M., Fazzuoli, M., Dini, A., Fanucci, F., Menna, F., Nirta, G., 2013. The Elba island: an intriguing geological puzzle in the northern Tyrrhenian sea. Geol. Field Trips SGI-ISPRA 5 (2.1). http://dx.doi.org/10.3301/GFT.2013.03.

Paynter, S., 2006. Regional variations in bloomery smelting slag of the Iron Age and Romano-British periods. Archaeometry 48, 271–292.

Pleiner, R., 2000. Iron in Archaeology: the European Bloomery Smelters. Archeologický ústav AVČR, Praha.

Rescic, S., 1998. Studio Archeometrico delle Scorie e dei Resti di Carica Mineraria Provenienti Dalla Necropoli del Casone (Populonia). Unpublished thesis. University of Florence.

Sauder, L., 2013. An American bloomery in sussex. In: Dungworth, D., Doonan, R. (Eds.), Accidental and Experimental Achaeometallurgy, HMS. Occasional Publication 7. Historical Metallurgy Society, London, pp. 69–74.

Schwab, R., Heger, D., HD., B., Pernicka, E., 2006. The provenance of iron artefacts from manching: a multi-technique approach. Archaeometry 48, 433–452.

Senn, M., Gfeller, U., Guénette-Beck, B., Lienemann, P., Ulrich, A., 2010. Tools to qualify experiments with bloomery furnaces. Archaeometry 52, 131–145.

Shapiro, L., Brannock, W., 1962. Rapid analyses of silicate, carbonate and phosphate rocks. Geol. Surv. Bull. 1144-A, 1–55.

Sperl, H.G., 1985. Untersuchungen zur Metallurgie der Etruscker. In: Martelli, M. (Ed.), L'Etruria mineraria, Proceedings of XII Convegno di Studi Etruschi e Italici, Firenze-Populonia-Piombino (Italy). Istituto di Studi Etruschi ed Italici, Leo S. Olschki Editore, Firenze, pp. 29–50.

Strillozzi, B., 1998. Studio di Scorie Ferrifere Etrusche della Zona di Baratti-Populonia. Unpublished thesis. University of Florence.

Tanelli, G., Benvenuti, M., Costagliola, P., Dini, A., Maineri, C., Mascaro, I., Lattanzi, P., Ruggieri, G., 2001. The iron mineral deposits of Elba Island: state of the art. Ofioliti 26, 239–248.

Tarassov, M., Mihailova, B., Tarassova, E., Konstantinov, L., 2002. Chemical composition and vibrational spectra of tungsten-bearing goethite and hematite from Western Rhodopes, Bulgaria. Eur. J. Mineral. 14, 977–986.

Voss, O., 1988. The iron production in Populonia. In: Sperl, G. (Ed.), The First Iron in the Mediterranean. PACT, Strasbourg, pp. 91–100.